

Supplementary information for

Synergistically enhanced photoelectrochemical properties of a layer-by-layer hybrid film based on graphene oxide and a free terpyridyl grafted ruthenium complex

Wei Yang, Ze-Bao Zheng, Ting-Ting Meng, Ke-Zhi Wang\*

Beijing Key Laboratory of Energy Conversion and Storage Materials, College of Chemistry, Beijing Normal University, Beijing 100875, P.R. China. Fax: +86-10-58802075; Tel: +86-10-58805476/62209940; E-mail: kzwang@bnu.edu.cn (K.-Z.Wang)

List of contents:

Preparation of the multilayer films

**Fig. S1** Scanning electron micrographs of (a) bare ITO, (b) ITO/(GO/Ru4)<sub>3</sub>GO film and (c) ITO/(GO/Ru4)<sub>4</sub> film at top view under 50,000 magnification.

**Fig. S2** Cyclic voltammograms of ITO/(GO/Ru4)<sub>1</sub> film in 0.1 M Na<sub>2</sub>SO<sub>4</sub> aqueous solution (pH = 2) at different scan rates. The inset is the peak I current dependence of scan rates.

**Fig. S3** Cyclic voltammograms of ITO/(GO/Ru(bpy)<sub>2</sub>(Htppip))<sub>n</sub> (n=1-6) films in 0.1 M Na<sub>2</sub>SO<sub>4</sub> electrolyte solution (pH=2) at a scan rate of 0.2V/s. The inset is the peak I current dependence of peak I currents on layer numbers.

**Fig. S10** Comparison of visible absorption spectra (solid line) with the photocurrent action spectrum (square) of ITO/(GO/Ru4)<sub>4</sub> film.

**Fig. S4** Cyclic voltammograms of ITO/(GO/Ru3)<sub>1</sub> film in 0.1 M TBAPF<sub>6</sub> CH<sub>2</sub>Cl<sub>2</sub> solution upon increasing scan rates from 0.05 to 10.0 V/s. The inset is the peak I current dependence on scan rates ( $v = 0.05\sim 1$  V/s).

**Fig. S5** The dependence of the cathodic and anodic overpotentials on the scan rates for ITO/(GO/Ru3)<sub>1</sub> film in 0.1 M TBAPF<sub>6</sub> CH<sub>2</sub>Cl<sub>2</sub> solution.

**Fig. S6** Dependence of photocurrent density produced by ITO/(GO/Ru4)<sub>1</sub> film on the concentrations of the electron donor hydroquinone in 0.1 M Na<sub>2</sub>SO<sub>4</sub> at an applied potential of -0.2 V versus SCE upon irradiation with 100 mW/cm<sup>2</sup> white light.

**Fig. S7** Dependence of photocurrent density produced by ITO/(GO/Ru4)<sub>1</sub> film on the concentrations of the electron acceptor K<sub>3</sub>Fe(CN)<sub>6</sub> in 0.1 M Na<sub>2</sub>SO<sub>4</sub> at an applied potential of -0.2 V versus SCE upon irradiation with 100 mW/cm<sup>2</sup> white light.

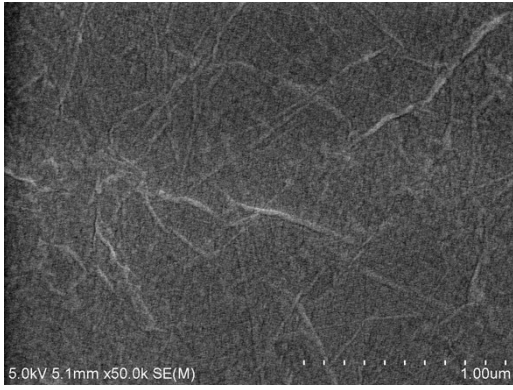
**Fig. S8** Photocurrent density changes induced by switching on and off the irradiation of ITO/(GO/Ru4)<sub>1</sub> film. The measurement was carried out at the potential of -0.2 V versus SCE in 0.1 M (a) air-equilibrated Na<sub>2</sub>SO<sub>4</sub> aqueous solution and (b) degassed Na<sub>2</sub>SO<sub>4</sub> aqueous solution by bubbling nitrogen for 10 min into the electrolyte solution.

**Fig. S9.** (a) Photocurrent changes induced by turning the irradiation on and off of ITO/(GO/Ru4)<sub>n</sub> (n = 1-6) films that were biased at -0.2 V vs. SCE. (b) Dependence of photocurrents of ITO/(GO/Ru4)<sub>n</sub> (n = 1-6) films on the number of layers.

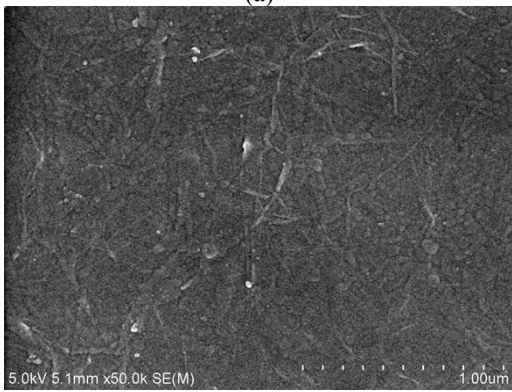
**Fig. S10** Comparison of visible absorption spectra (solid line) with the photocurrent action spectrum (square) of ITO/(GO/Ru4)<sub>4</sub> film.

### Preparation of the multilayer films

The thin film fabrication procedures are schematically illustrated in Fig. 2. The quartz or ITO substrates were cleaned sequentially by sonication in detergent, washing with copious water, and soaking in Piranha solution (v/v 3:1, concentrated H<sub>2</sub>SO<sub>4</sub>/30% H<sub>2</sub>O<sub>2</sub>) for the glass substrate or a mixed solution (v/v/v 1:1:5, 25% NH<sub>3</sub>·H<sub>2</sub>O/30% H<sub>2</sub>O<sub>2</sub>/DI water) for 40 min. *Piranha solution is highly corrosive and powerful oxidizing agent. It should be handled with extreme caution in order to avoid inhalation and contacts with skin and eyes.* After the cleaned substrates were then subjected to following treatments: (I) silanization with a 3-aminopropyltriethoxysilane/ethanol (5:95, v/v) solution for 12 h at room temperature made the surface of the substrate covered with the amino groups. (II) The amino covered substrates were protonated by contacting with an aqueous HCl solution (pH ≈ 3) for 10 min. (III) The protonated substrates were immersed into a 1 mg/mL GO aqueous solution for 15 min, and were washed carefully with ethanol and DI water, produced the substrates covered with negatively charged GO on the surface. (IV) The GO deposited substrates were immersed in a 0.5 mM **Ru4**(ClO<sub>4</sub>)<sub>2</sub> aqueous solution for 15 min, and were rinsed with ethanol and DI water carefully, and air-blow dried. Repetition of steps III and IV for *n* times afforded the multilayer films (GO/**Ru4**)<sub>*n*</sub> on the both sides of the substrates.



(a)



(b)

**Fig. S1** Scanning electron micrographs of (a) ITO/(GO/Ru4)<sub>3</sub>GO film and (b) ITO/(GO/Ru4)<sub>4</sub> film at top view under 50,000 magnification.

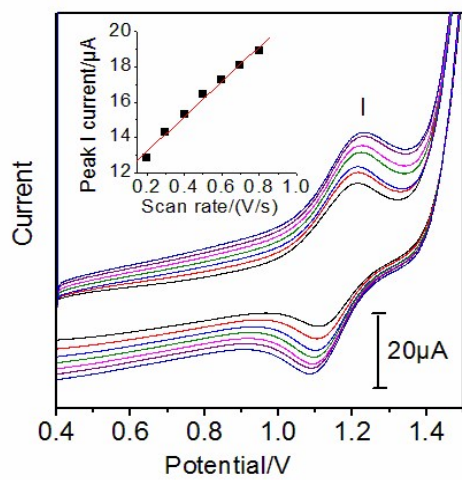


**Fig. S2** Cyclic voltammograms of ITO/(GO/Ru4)<sub>1</sub> film in 0.1 M Na<sub>2</sub>SO<sub>4</sub> aqueous solution (pH = 2) at different scan rates. The inset is the peak I current dependence of scan rates.

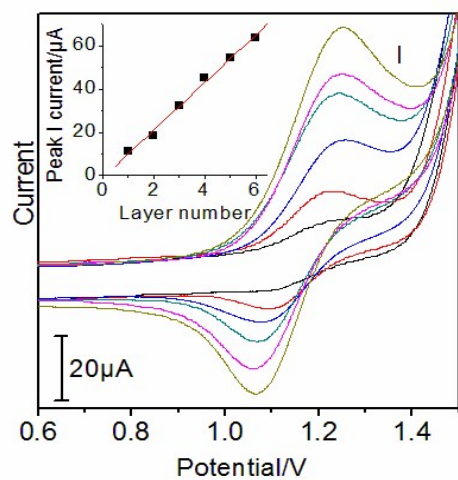


**Fig. S3** Cyclic voltammograms of ITO/(GO/Ru4)<sub>n</sub> (n = 1-6) films in 0.1 M Na<sub>2</sub>SO<sub>4</sub> electrolyte solution (pH = 2) at a scan rate of 0.2V/s. The inset is the peak I current dependence of peak I currents on layer numbers.

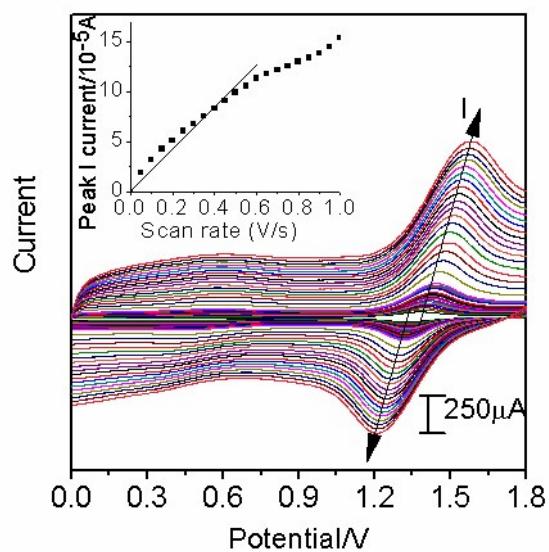


**Fig. S4** Cyclic voltammograms of ITO/(GO/Ru<sub>3</sub>)<sub>1</sub> film in 0.1 M TBAPF<sub>6</sub> CH<sub>2</sub>Cl<sub>2</sub> solution upon increasing scan rates from 0.05 to 10.0 V/s. The inset is the peak I current dependence on scan rates ( $v = 0.05\sim 1$  V/s).

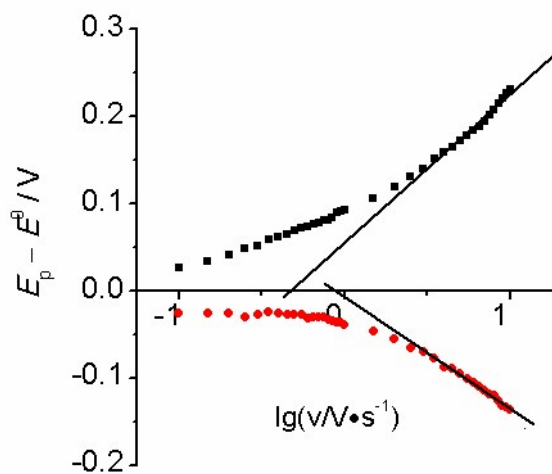


**Fig. S5** The dependence of the cathodic and anodic overpotentials on the scan rates for ITO/(GO/Ru3)<sub>1</sub> film in 0.1 M TBAPF<sub>6</sub> CH<sub>2</sub>Cl<sub>2</sub> solution.

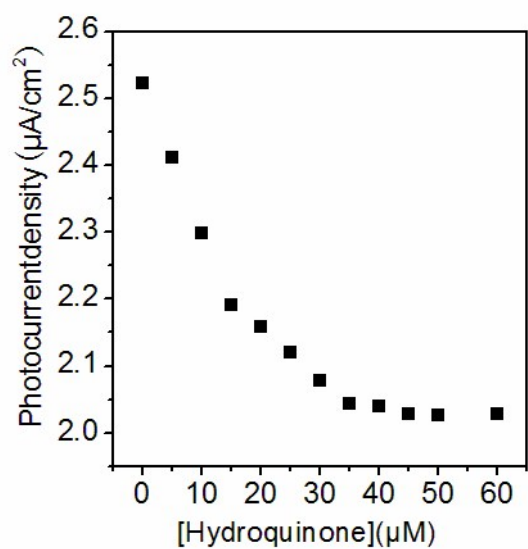


**Fig. S6** Dependence of photocurrent density produced by ITO/(GO/Ru4)<sub>1</sub> film on the concentrations of the electron donor hydroquinone in 0.1 M Na<sub>2</sub>SO<sub>4</sub> at an applied potential of -0.2 V versus SCE upon irradiation with 100 mW/cm<sup>2</sup> white light.



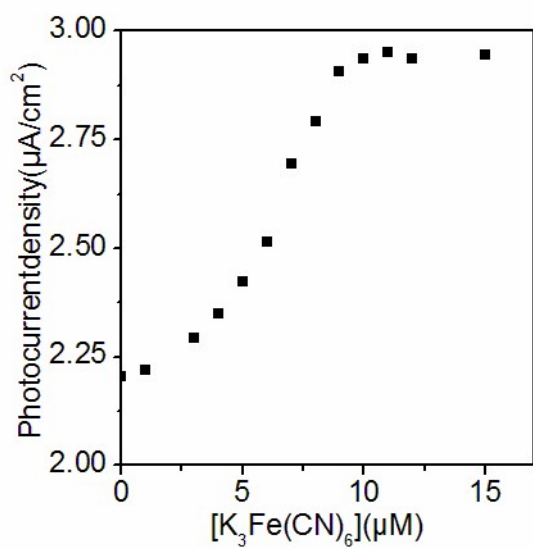


**Fig. S7** Dependence of photocurrent density produced by ITO/(GO/Ru4)<sub>1</sub> film on the concentrations of the electron acceptor K<sub>3</sub>Fe(CN)<sub>6</sub> in 0.1 M Na<sub>2</sub>SO<sub>4</sub> at an applied potential of -0.2 V versus SCE upon irradiation with 100 mW/cm<sup>2</sup> white light.

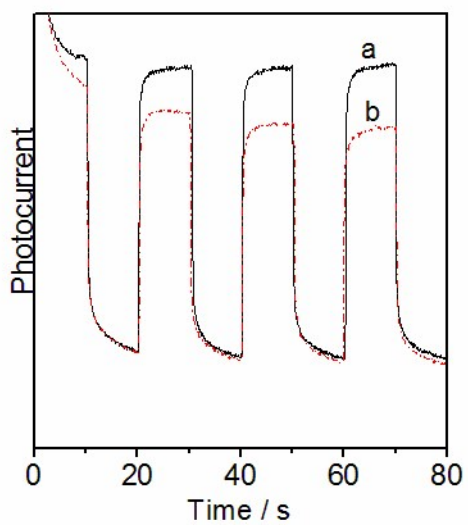


**Fig. S8** Photocurrent density changes induced by switching on and off the irradiation of ITO/(GO/Ru4)<sub>1</sub> film. The measurement was carried out at the potential of  $-0.2$  V versus SCE in  $0.1$  M (a) air-equilibrated Na<sub>2</sub>SO<sub>4</sub> aqueous solution and (b) degassed Na<sub>2</sub>SO<sub>4</sub> aqueous solution by bubbling nitrogen for 10 min into the electrolyte solution.

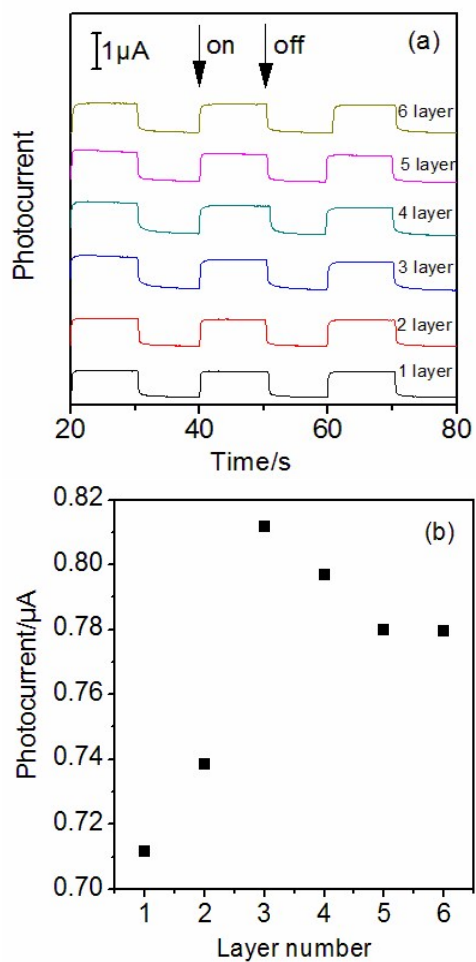


**Fig. S9.** (a) Photocurrent changes induced by turning the irradiation on and off of ITO/(GO/Ru4)<sub>n</sub> (*n* = 1-6) films that were biased at -0.2 V vs. SCE. (b) Dependence of photocurrents of ITO/(GO/Ru4)<sub>n</sub> (*n* = 1-6) films on the number of layers.

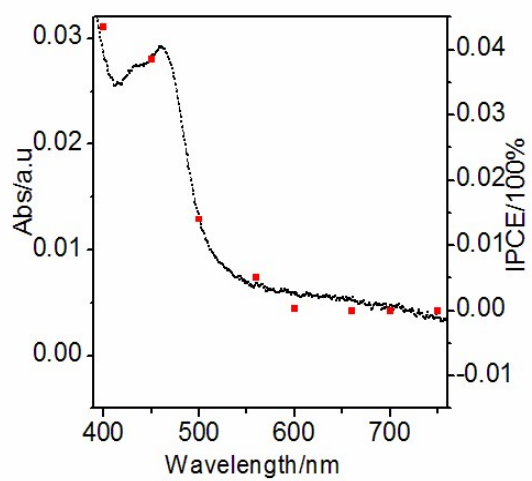


**Fig. S10** Comparison of visible absorption spectra (solid line) with the photocurrent action spectrum (square) of ITO/(GO/Ru4)<sub>4</sub> film.